A fast and robust minimum entropy based non-interactive Nyquist ghost correction algorithm

S. Skare[1], D. B. Clayton[1], R. Newbould[1], M. Moseley[1], R. Bammer[1]

[1]Radiology, Stanford University, Palo Alto, CA, United States

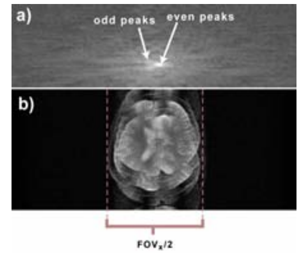

Figure 1 a) k-space (w/ ramp sampling) acquired with 4-shot EPI. Additional odd/even echo misalignment was introduced this work. b) Reconstructed image from a), omitting ramp sampling correction. About half FOV in readout direction is outside the object, which cannot drive the search towards the minimum.

Introduction. Nyquist ghosting occurs in EPI due to misalignment between odd and even echoes. For this reason, clinical EPI scans are commonly performed with an additional reference scan from which phase information can be used to correct ghosting errors. For multi-shot, multi-coil and multi-slice acquisitions, this additional scan can rival imaging time. Alternatives to reference scans are post-processing methods that require no additional information. One such method (1) minimizes the intensity in a ROI selected in the ghost area by iteratively refining phase parameters, however, this method requires user interaction. Another elegant method (2) uses the total image entropy as a cost function for iterative optimization and makes no assumptions about the shape or size of the object being imaged. However, the computation time to correct a 64-slice 128×128 4-shot data set has been reported to be 2.5 min. A clinically viable replacement for the reference scan may never fail, regardless of acquisition parameters chosen, anatomy of interest and how well the system is calibrated. Here we present a robust iterative entropy minimization implementation for ghost removal that we now use routinely as a replacement for reference scanning in clinical single- and multi-shot, GRAPPA-accelerated DWI and PWI EPI exams.

Materials and Methods. Minimizing the entropy, $E = -\Sigma\ B/\log(B)$; $B_{ij} = I_{ij}/\Sigma\ I_{ij}^2$, of a magnitude image has the effect of confining signal to as few pixels as possible. An image with some degree of ghosting (Fig. 1b) has, therefore, higher entropy than one without ghosting. Minimizing E by varying the constant and linear phase terms, $\mathbf{\Phi} = [\phi_{on}\ \phi_{ln}]$, can correct the differences between the odd and even echoes, minimizing the ghosting. Our algorithm proceeds as follows: Perform an initial 1D FT^{-1} to x-k_y space. Start the iterative search at $\mathbf{\Phi_0} = [\phi_{on,0}\ \phi_{ln,0}]$., and perform the following iterative loop: (a) apply phase map (given by $\mathbf{\Phi}$) on odd and even echoes, (b) perform a 1D FT^{-1} in the k_y direction, and (c) calculate the entropy E of the magnitude image I. As the E is π-periodic w.r.t. ϕ_{on} (see Fig. 2) we are using a semi-bounded search algorithm, in this case Gauss-Newton. The algorithm operates prior to regridding due to ramp sampling. This was implemented in Matlab on a 3 GHz Linux pc. *ROBUSTNESS:* In Fig. 2, $E(I,\mathbf{\Phi})$ is shown for 1 to 4 shot EPI brain data (Fig. 1b is a 4-shot case). Only if the ghosting is small, one will start searching in the quadratic region close to the global solution (black arrows), the width of which corresponds roughly to ½ pixel shift, or about 1 μs time delay between odd/even echoes. From our clinical experience, this is seldom the case; even though ghosting levels of 8 pixels as in Fig. 1 are rarely encountered. With the topology shown in Fig. 2, derivative based search algorithms like Gauss-Newton are not guaranteed to reach the global minimum. To assure that minimization starts within the narrow quadratic region near the solution, we have chosen to calculate $E(I,\mathbf{\Phi})$ on a grid prior to iteration. A suitable grid size was found to be ϕ_{on}: -1.6 to 1.6 in 5 steps, and ϕ_{ln} = -10 to 10 in 21 steps (corresponding to extremes of ±2×10 pixels shift or 40 μs between odd/even echoes). $\mathbf{\Phi_0} = [\phi_{on,0}\ \phi_{ln,0}]$ was chosen for the smallest E on the grid. *SPEED:* From our experience, $\mathbf{\Phi}$ does not vary significantly between coils or slices; hence for a fast implementation, $\mathbf{\Phi}$ can be determined once from an average coil image of the center slice in the volume (on the b=0 image for DWI). To further increase speed, we have performed the ghost correction with various image resolutions and with full and half FOV_x. The rationale for the latter may be seen in the uncorrected image without regridding (Fig 1b), where there is little information in the image outside the central $FOV_x/2$. Using the central part of image space during the estimation of $\mathbf{\Phi}$ corresponds to using every other readout point in k-space. Image acquisition was performed on a volunteer on a 1.5T GE HD system (GEHC, Milwaukee, WI) with 50 mT/m gradients using a DW-EPI sequence with 1-4 shots, 128×80(128) half Fourier acquisition and FOV = 24×24 cm. Odd/even misalignments were introduced post-acquisition to enforce a robust correction strategy.

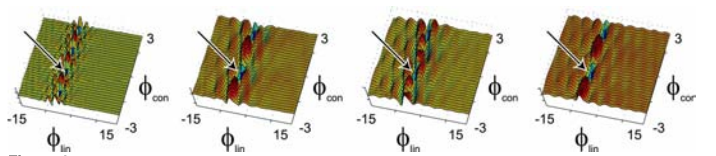

Figure 2
The entropy metric as a function of $\mathbf{\Phi} = [\phi_{on}\ \phi_{ln}]$ for a) 1-shot, b) 2-shot, c) 3-shot and d) 4-shot EPI. True solution is indicated with the arrow. These surface plots show that the entropy metric is only a smooth quadratic function very close to the true minimum. If the MR-system is not well calibrated (i.e. close to the solution), it is easy to get trapped in a local minimum. The function is π-periodic in the ϕ_{on} dimension, why a semi-constrained search is adequate.

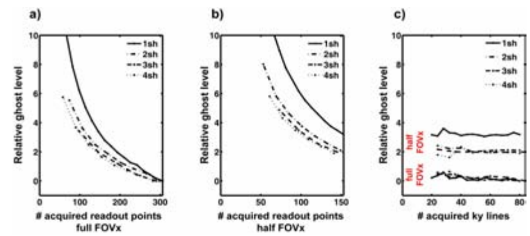

Figure 3
Sum-of-squares difference (SSD) between image corrected using all data and reduced/cropped data. 1-4 shot acquisitions are shown. a) SSD vs. # readout points used. b) as a), but also with skipping every other point in kx (=> half image FOVx). c) SSD vs. # ky lines using i) full FOVx, and ii) half FOVx.

Results. The k-space data in Fig. 3a-d, corresponding to 1 through 4 shot EPI, was first corrected using all data, which is presented in Fig. 3e-h. The time for convergence was only 2.1 seconds including the pre-processing step. In Fig 2, the penalty of removing k-space data in the interest of speed is presented. For any number of shots, the number of ky lines could be reduced to 24 (Fig. 2c) without affecting the ghosting level. Reducing resolution in the x-direction by an equal amount had a bad impact on the ghosting situation (Fig. 2a-b). However, keeping the x-resolution (or $k_{x,max}$) while reducing FOVx to half, did not affect $\mathbf{\Phi}$ significantly. In Fig. 3i-l, corrected images are shown using 24 ky lines, full x-resolution and half FOV_x. Computation time in this case was only 0.3 seconds.

Discussion. We have shown that it is possible to correct for Nyquist ghosting in about 0.3 seconds in Matlab on single- and multi-shot T2w EPI. Assuming no motion between shots, this method works equally fast and well for single and multi-shot EPI data since the search space remains the same, the only difference is in which lines of k-space need to be adjusted. The robustness lies mostly in the choice of good starting guess $\mathbf{\Phi_0}$, which also makes the convergence faster. Because the slice-to-slice variation was observed to be small for all the cases studied, it was sufficient to estimate $\mathbf{\Phi}$ on the center slice and apply it to all other slices. Slight improvement for edge slices may be obtained in some cases by also estimate $\mathbf{\Phi}$ on one of the outer slices, but was not found necessary for the clinical routine. Without affecting the residual ghosting level, it was possible to reduce the computational time from 2 to 0.3 sec by using every other k_x point ($FOV_x/2$) and only 24 k_y points in k-space. This algorithm makes no assumptions about the object shape, works equally well for single- and multi-shot data, and does not require user input. The only restriction is that it cannot be used if the object is aliased in the phase encoding direction if FOV_y is too small.

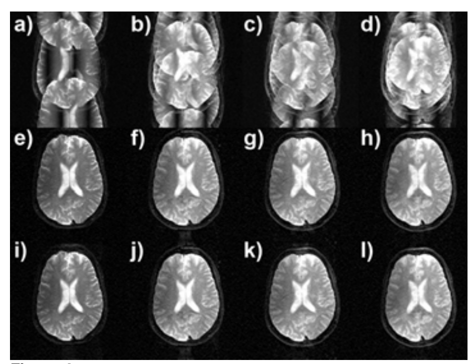

Figure 4
Images before and after ghost correction. Columns are (left to right): 1-4 shots. Top panel (a-d) shows images before correction. Mid panel (e-h) shows images after correction using all k-space data. Bottom panel (i-l) shows the images after correction using half FOVx and only 24 out of 80 ky lines for speed purposes. Subtle residual ghosting in f,g,j,k is due to motion between shots, which we currently don't model.

References: 1) Buonocore MH, Zhu DC. Magn Reson Med 2001;45(1):96-108. 2) Clare. 2003; Toronto. p 1041.

Acknowledgements: This work was supported in part by NIH-1R01NS35959, NIH-1R01EB002771, Lucas Foundation, Center of Advanced MR Technology of Stanford (NCRR P41 RR 09784)